



# Slow Crack Growth of Brittle Materials With Exponential Crack-Velocity Formulation— Part 3: Constant Stress and Cyclic Stress Experiments

Sung R. Choi  
Ohio Aerospace Institute, Brook Park, Ohio

Noel N. Nemeth and John P. Gyekenyesi  
Glenn Research Center, Cleveland, Ohio

## The NASA STI Program Office . . . in Profile

Since its founding, NASA has been dedicated to the advancement of aeronautics and space science. The NASA Scientific and Technical Information (STI) Program Office plays a key part in helping NASA maintain this important role.

The NASA STI Program Office is operated by Langley Research Center, the Lead Center for NASA's scientific and technical information. The NASA STI Program Office provides access to the NASA STI Database, the largest collection of aeronautical and space science STI in the world. The Program Office is also NASA's institutional mechanism for disseminating the results of its research and development activities. These results are published by NASA in the NASA STI Report Series, which includes the following report types:

- **TECHNICAL PUBLICATION.** Reports of completed research or a major significant phase of research that present the results of NASA programs and include extensive data or theoretical analysis. Includes compilations of significant scientific and technical data and information deemed to be of continuing reference value. NASA's counterpart of peer-reviewed formal professional papers but has less stringent limitations on manuscript length and extent of graphic presentations.
- **TECHNICAL MEMORANDUM.** Scientific and technical findings that are preliminary or of specialized interest, e.g., quick release reports, working papers, and bibliographies that contain minimal annotation. Does not contain extensive analysis.
- **CONTRACTOR REPORT.** Scientific and technical findings by NASA-sponsored contractors and grantees.

- **CONFERENCE PUBLICATION.** Collected papers from scientific and technical conferences, symposia, seminars, or other meetings sponsored or cosponsored by NASA.
- **SPECIAL PUBLICATION.** Scientific, technical, or historical information from NASA programs, projects, and missions, often concerned with subjects having substantial public interest.
- **TECHNICAL TRANSLATION.** English-language translations of foreign scientific and technical material pertinent to NASA's mission.

Specialized services that complement the STI Program Office's diverse offerings include creating custom thesauri, building customized data bases, organizing and publishing research results . . . even providing videos.

For more information about the NASA STI Program Office, see the following:

- Access the NASA STI Program Home Page at <http://www.sti.nasa.gov>
- E-mail your question via the Internet to [help@sti.nasa.gov](mailto:help@sti.nasa.gov)
- Fax your question to the NASA Access Help Desk at 301-621-0134
- Telephone the NASA Access Help Desk at 301-621-0390
- Write to:  
NASA Access Help Desk  
NASA Center for AeroSpace Information  
7121 Standard Drive  
Hanover, MD 21076



# Slow Crack Growth of Brittle Materials With Exponential Crack-Velocity Formulation— Part 3: Constant Stress and Cyclic Stress Experiments

Sung R. Choi  
Ohio Aerospace Institute, Brook Park, Ohio

Noel N. Nemeth and John P. Gyekenyesi  
Glenn Research Center, Cleveland, Ohio

National Aeronautics and  
Space Administration

Glenn Research Center

This report is a formal draft or working paper, intended to solicit comments and ideas from a technical peer group.

The Aerospace Propulsion and Power Program at NASA Glenn Research Center sponsored this work.

Available from

NASA Center for Aerospace Information  
7121 Standard Drive  
Hanover, MD 21076

National Technical Information Service  
5285 Port Royal Road  
Springfield, VA 22100

Available electronically at <http://gltrs.grc.nasa.gov/GLTRS>

# **Slow Crack Growth of Brittle Materials With Exponential Crack-Velocity Formulation—Part 3: Constant Stress and Cyclic Stress Experiments**

Sung R. Choi  
Ohio Aerospace Institute  
Brook Park, Ohio 44142

Noel N. Nemeth and John P. Gyekenyesi  
National Aeronautics and Space Administration  
Glenn Research Center  
Cleveland, Ohio 44135

## **Summary**

The previously determined life prediction analysis based on an exponential crack-velocity formulation was examined using a variety of experimental data on advanced structural ceramics tested under constant stress and cyclic stress loading at ambient and elevated temperatures. The data fit to the relation between the time to failure and applied stress (or maximum applied stress in cyclic loading) was very reasonable for most of the materials studied. It was also found that life prediction for cyclic stress loading from data of constant stress loading in the exponential formulation was in good agreement with the experimental data, resulting in a similar degree of accuracy as compared with the power-law formulation. The major limitation in the exponential crack-velocity formulation, however, was that the inert strength of a material must be known a priori to evaluate the important slow-crack-growth (SCG) parameter  $n$ , a significant drawback as compared with the conventional power-law crack-velocity formulation.

## **Introduction**

Advanced ceramics are candidate materials for structural applications in advanced heat engines and heat recovery systems. The major limitation of these materials in hostile environments, particularly at elevated temperatures, is slow-crack-growth (SCG)-associated failure, where slow crack growth of inherent defects or flaws can occur until a critical size for catastrophic failure is reached. To ensure accurate life prediction of ceramic components, it is important to accurately evaluate SCG parameters of a material with specified loading and environmental conditions.

Life prediction (or SCG) parameters of a material depend on what type of crack-velocity formulation is used to determine them. The power-law crack-velocity formulation has been used for several decades to describe SCG behavior of a variety of brittle materials ranging from glass to glass ceramics to advanced structural ceramics. The primary advantage of the power-law formulation over other crack-velocity formulations is the simplicity in its mathematical expression for lifetime analysis. It has also been observed that the power-law formulation has adequately described the SCG behavior of many brittle materials. Because of these merits, the power-law formulation has been used in two recent ASTM test standards (refs. 1 and 2) to determine SCG parameters of advanced ceramics in constant stress rate testing at both ambient and elevated temperatures. Alternative crack-velocity formulations take exponential forms to account for the influence of other phenomena (such as a corrosion reaction, diffusion control, thermal activation, etc.). However, these exponential forms in general do not result in simple mathematical expressions of life prediction formulation, although the forms might better represent the actual SCG behavior of some materials. Because of this mathematical inconvenience, the exponential crack-velocity formulation has rarely been used for brittle materials as a means of life prediction methodology in testing or analysis.

In part 1 of this report (ref. 3), the exponential crack-velocity formulation was analyzed to achieve a more convenient and simplified life prediction analysis using three widely utilized load configurations including constant stress rate (dynamic fatigue), constant stress (static fatigue), and cyclic stress (cyclic fatigue). The resulting analysis obtained with the exponential formulation was compared with that of the power-law formulation to assess which would yield a better life prediction methodology in terms of accuracy and convenience. The analysis of constant stress rate loading was scrutinized in part 2 of this report (ref. 4) using a variety of experimental data on constant stress rate and preloading tests at both ambient and elevated temperatures. The overall accuracy of analysis in conjunction with experimental data was very reasonable; however, the requirement of having accurate inert strength data to determine the major SCG parameter  $n$  gave rise to a significant limitation in using the exponential formulation rather than the conventional power-law formulation. As an extension of previous work (refs. 3 and 4), this report will describe the exponential formulation and its experimental verification in both constant stress and cyclic stress loading configurations. The SCG data for various advanced ceramics at both ambient and elevated temperatures were utilized for this purpose in terms of the degree of data fitting as well as of the accuracy of life prediction from one loading configuration to another.

All symbols used in this report are listed in the appendix.

This work was sponsored in part by the High Operating Temperature Propulsion Components (HOTPC) and the Zero CO<sub>2</sub> Emission Technology (ZCET) projects at the NASA Glenn Research Center, Cleveland, Ohio.

## Theoretical Background

The results of the previous SCG analysis (ref. 3) using the exponential crack-velocity formulation will be briefly presented in this section for the cases of constant stress and cyclic stress loading. The companion SCG analysis using the conventional power-law velocity formulation will also be included here for comparison and generalization of the analysis.

### Power-Law SCG Formulation

The widely utilized empirical power-law crack velocity above the fatigue limit is expressed in the following familiar form:

$$v = \frac{da}{dt} = A \left( \frac{K_I}{K_{IC}} \right)^n \quad (1)$$

where

$v$	crack velocity
$a$	crack size
$t$	time
$K_I$	mode I stress intensity factor
$K_{IC}$	mode I critical stress intensity factor (or fracture toughness)
$A, n$	material- and environment-dependent SCG parameters

Constant stress and cyclic stress testing are performed by applying, respectively, constant stress and cyclic stress to ground-test specimens to determine the corresponding time to failure. The time to failure in constant stress and cyclic stress tests can be analytically derived to give the following familiar relations (refs. 5 and 6):

$$t_{fs} = D_s \sigma^{-n} \quad (2)$$

$$t_{fc} = D_c \sigma_{\max}^{-n} \quad (3)$$

where  $t_{fs}$  is time to failure in constant stress testing subjected to a constant applied stress  $\sigma$ , and  $t_{fc}$  is time to failure in cyclic stress testing whereby the material is subjected to cyclic loading with a maximum stress  $\sigma_{\max}$ . The parameters  $D$  can be expressed as follows (refs. 5 and 6):

$$D_s = BS_i^{n-2} \quad (4)$$

$$D_c = \frac{BS_i^{n-2}}{\frac{1}{\tau} \int_0^\tau [f(t)]^n dt} \quad (5)$$

where  $S_i$  is the inert strength whereby no slow crack growth occurs;  $B = 2K_{IC}/AY^2(n-2)$  where  $Y$  is the crack geometry factor in the relation of  $K_I = Y\sigma a^{1/2}$  where  $\sigma$  is remote applied stress;  $f(t)$  is a periodic function in cyclic loading specified in  $\sigma(t) = \sigma_{\max} f(t)$  in a range of  $0 \leq f(t) \leq 1$ ; and  $\tau$  is the period. The slow-crack-growth parameters  $n$  and  $D$  (and  $B$  or  $A$ ) can be obtained by a linear regression analysis with experimental data in conjunction with the corresponding equation, (2) or (3), depending on the type of loading. Hence, it is straightforward to determine SCG parameters  $n$  and  $D$  by least-squares fitting of the data, which is the most advantageous feature of the power-law crack-velocity formulation. This convenience and merit in mathematical simplicity in addition to the use of routine test techniques have led for several decades to the almost exclusive use of the power-law crack-velocity formulation in life prediction analysis and testing for many brittle materials over a wide range of temperatures.

### Exponential SCG Formulation

Several exponential crack-velocity formulations that have been previously proposed are based on other factors including chemically assisted corrosion reaction (ref. 7), diffusion-controlled stress rupture (ref. 8), thermally activated process (ref. 9), chemical reaction with constant crack-tip configuration (ref. 10), kinetic crack growth (ref. 11), and others (ref. 12). The generalized exponential crack-velocity forms thus proposed are

$$v = A \exp \left[ n \left( \frac{K_I}{K_{IC}} \right) \right] \quad (6)$$

$$v = A \left( \frac{K_I}{K_{IC}} \right) \exp \left[ n \left( \frac{K_I}{K_{IC}} \right) \right] \quad (7)$$

$$v = A \left( \frac{K_{IC}}{K_I} \right) \exp \left[ n \left( \frac{K_I}{K_{IC}} \right) \right] \quad (8)$$

$$v = A \exp \left[ n \left( \frac{K_I}{K_{IC}} \right)^2 \right] \quad (9)$$

$$v = A \left( \frac{K_I}{K_{IC}} \right) \exp \left[ n \left( \frac{K_I}{K_{IC}} \right)^2 \right] \quad (10)$$

where  $A$  and  $n$  are SCG parameters and are different from those used in the power-law formulation.

Unlike the power-law crack-velocity formulation, the exponential crack-velocity forms do not yield simple analytical expressions either of the resulting strength as a function of applied stress rate in constant stress rate testing or of the resulting time to failure as a function of the applied stress in constant stress testing or the maximum applied stress in cyclic stress testing. Several attempts have been made under both constant stress rate and constant stress loading to obtain corresponding lifetime expressions through numerical integration incorporating with linear (refs. 13 and 14) or nonlinear (ref. 15) regression analysis. However, this approach still involves complexity in regression technique, as compared to the simple least-squares approach in the power-law formulation.

Slow crack growth analyses of three load configurations of constant stress rate, constant stress, and cyclic stress loading were made in the previous work (ref. 3). More convenient, simpler formulations were obtained through numerical approaches. It was found that little difference in SCG formulation existed among equations (6) to (8) and that equation (6) was regarded as a representative exponential crack-velocity form. Hence, equation (6) was exclusively used in the previous analysis. To minimize the number of parameters to be specified (such as  $A$ ,  $a$ ,  $\sigma$ ,  $S_i$ ,  $K_{IC}$ , and  $t$ ), it is convenient to use a normalized scheme, as used previously for the power-law velocity formulation (refs. 16 to 18):

$$K^* = \frac{K_I}{K_{IC}}; \quad T^* = \frac{A}{a_i} t; \quad C^* = \frac{a}{a_i}; \quad \sigma^* = \frac{\sigma}{S_i}; \quad \sigma_{\max}^* = \frac{\sigma_{\max}}{S_i} \quad (11)$$

where

$K^*$	stress intensity factor (SIF)
$T^*$	time
$C^*$	crack size
$\sigma^*$	applied stress
$\sigma_{\max}^*$	applied maximum stress



and  $a_i$  is the critical crack size in the inert condition or is the initial crack size. Using these variables, the exponential crack-velocity equation (6) can be normalized as

$$\frac{dC^*}{dT^*} = e^{nK^*} \quad (12)$$

The corresponding normalized SIF,  $K^*$  is expressed in constant stress and in sinusoidal cyclic loading, respectively, as follows:

$$K^* = \sigma^* (C^*)^{1/2} \quad (13)$$

$$K^* = \left\{ \frac{1+R}{2} + \frac{1-R}{2} \sin \left[ \left( \frac{\omega a_i}{A} \right) T^* \right] \right\} \sigma_{\max}^* (C^*)^{1/2} \quad (14)$$

where  $R$  is the stress (or load) ratio, defined as  $R = \sigma_{\min}/\sigma_{\max}$ , where  $\sigma_{\min}$  and  $\sigma_{\max}$  are the minimum and maximum applied stresses, respectively, in sinusoidal cyclic loading, and  $\omega$  is the angular velocity. As typical of ceramics, the crack size at instability in either an inert or fatigue environment was assumed to be small compared with the body of the specimens or components (i.e., an infinite-body assumption). The differential equation (12) was solved numerically using a fourth-order Runge-Kutta method for each respective loading configuration. The initial condition was  $C^* = 1.0$  at  $T^* = 0$ , and the instability condition was  $K^* = 1.0$  and  $dK^*/dC^* > 0$ . In cyclic loading, the frequency was taken as arbitrary values of  $\omega a_i/A \geq 10^8$ , depending on the values of maximum applied stress and  $n$ . The effect of frequency on solution was found to be independent in part 1 of this study (ref. 3).

**Constant stress loading.**—The numerical results of normalized time to failure  $T_f^*$  as a function of normalized applied stress  $\sigma^*$  are shown in figure 1, where  $\ln T_f^*$  was plotted against  $\sigma^*$  for values of  $n$  ranging from 5 to 100. The general trend of the solution can be summarized in terms of the convergence of  $\ln T_f^*$  close to zero with  $\sigma^* \rightarrow 0$ , the increased SCG susceptibility with decreasing  $n$  values, and the linearity between  $\ln T_f^*$  and  $\sigma^*$  in the range of  $\sigma^*$  from 0.2 to 0.9. As a consequence, the relationship between normalized time to failure and normalized applied stress within the linear region can be written as

$$\ln T_f^* = -n' \sigma^* + \beta \quad (15)$$

where  $n'$  is the slope or apparent (calculated) SCG parameter, and  $\beta$  is the intercept. The linearity between  $\ln T_f^*$  and  $\sigma^*$  was obvious when the correlation coefficient of  $r^2 \geq 0.995$  for each curve was considered. Hence, the slope  $n'$  and intercept  $\beta$  can be determined with reasonable accuracy by a linear regression analysis of the numerical results based on equation (15). The relationship between the calculated apparent SCG parameter  $n'$  and the true SCG parameter  $n$  (an input datum) is

$$n' = 0.9827n + 3.3440 \quad (16)$$

with  $r^2 = 0.9997$ . The difference between  $n'$  and  $n$  was  $\geq 8$  percent for  $n \leq 30$  and  $\leq 5$  percent for  $n \geq 40$  so that a further approximation of equation (16) is made for the case of  $n \geq 40$  as follows:

$$n' \approx n \quad (17)$$

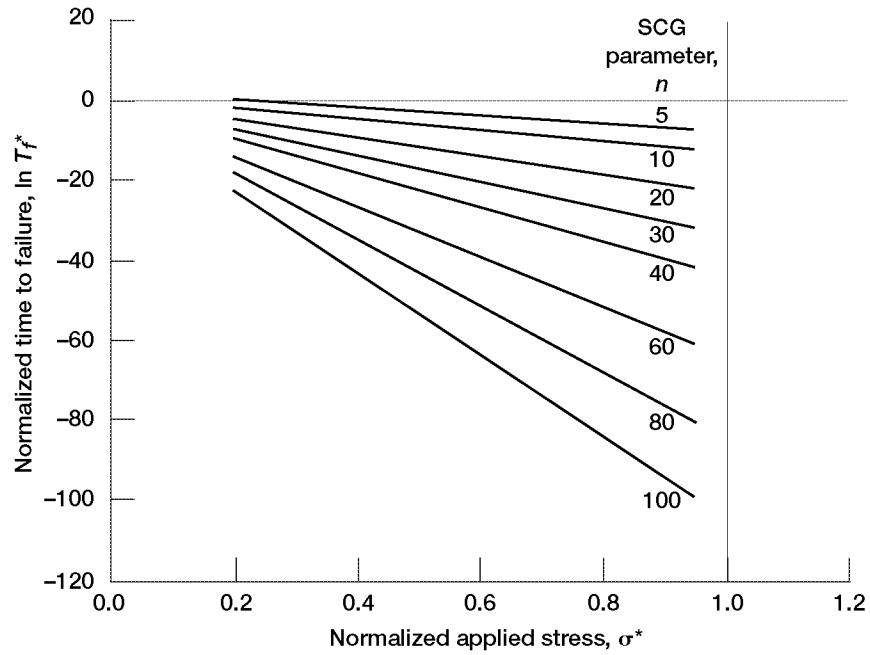


Figure 1.—Numerical results of normalized time to failure  $T_f^*$  as function of normalized applied stress  $\sigma^*$  in constant stress loading for different values of SCG parameters  $n$  in exponential crack-velocity formulation.

The intercept  $\beta$  is dependent on  $n$ :

$$\beta = -1.913 + 4.985 e^{-0.049n} \quad (18)$$

with  $r^2 = 0.9907$ .

For the nonnormalized expression, equation (11) is used to reduce equation (15) to

$$\ln t_f = -n' \frac{\sigma}{S_i} + \chi \quad (19)$$

where  $t_f$  is time to failure and

$$\chi = \ln\left(\frac{a_i}{A}\right) + \beta \quad (20)$$

Therefore, the SCG parameters  $n'$  and  $\chi$  in constant stress loading can be obtained from the slope and intercept, respectively, by a simple linear regression analysis of experimental data of  $\ln t_f$  as a function of  $\sigma$  or  $\sigma/S_i$ . With  $n'$  determined, the true SCG parameter  $n$  can be evaluated from equation (16). The SCG parameter  $A$  can be estimated from equation (20) from calculated  $\chi$  together with  $\beta$  (eq. (18)) and a known value of  $a_i$ . A notable difference in constant stress loading between the power-law and exponential formulations is that in the power-law formulation,  $t_f$  is a function of  $\sigma$  as seen in equation

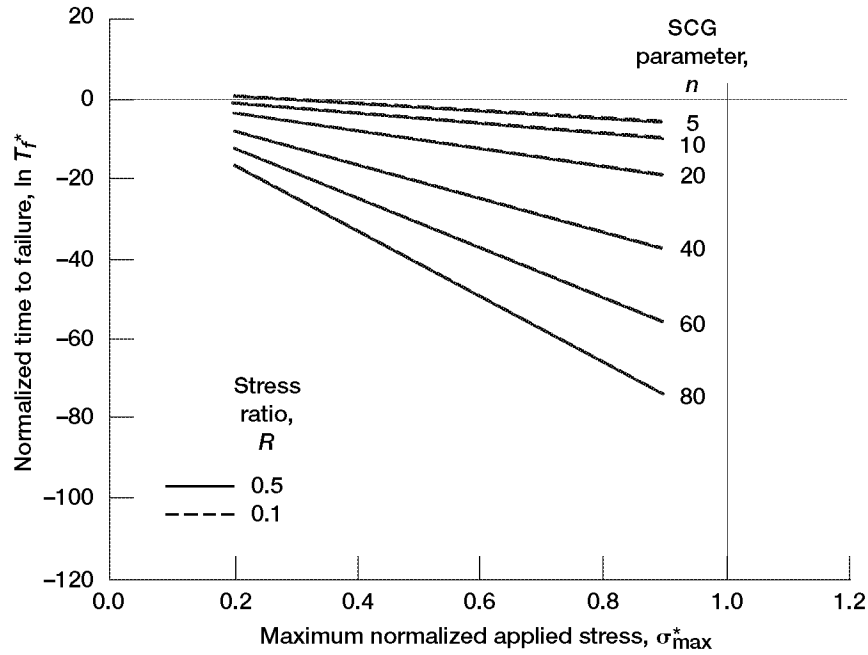


Figure 2.—Numerical results of normalized time to failure  $T_f^*$  as function of normalized maximum applied stress  $\sigma_{\max}^*$  in sinusoidal cyclic loading for different values of SCG parameters  $n$  in exponential crack-velocity formulation.

(2); however, in the exponential formulation,  $\ln t_f$  is a function of  $\sigma$  or  $\sigma/S_i$  as seen in equation (19). Hence, inert strength must be known to determine the major SCG parameter  $n$ , which would be a distinctive drawback of the exponential formulation compared with the conventional power-law formulation.

**Cyclic stress loading.**—The results of the numerical solution of normalized time to failure  $T_f^*$  as a function of maximum normalized applied stress  $\sigma_{\max}^*$  in sinusoidal cyclic loading with stress ratios  $R = 0.1$  and  $0.5$  are shown in figure 2, where  $\ln T_f^*$  was plotted against  $\sigma_{\max}^*$  for values of  $n$  ranging from 5 to 80. Similar to the case of constant stress loading,  $\ln T_f^*$  is linear with respect to  $\sigma_{\max}^*$  in the range 0.2 to 0.9 and converges close to zero with further decreasing maximum normalized applied stress. The linearity between  $\ln T_f^*$  and  $\sigma_{\max}^*$  is evident considering that the correlation coefficient  $r^2 \geq 0.997$ . Hence, the relationship between  $\ln T_f^*$  and  $\sigma_{\max}^*$  can be expressed as

$$\ln T_f^* = -n' \sigma_{\max}^* + \beta \quad (21)$$

where  $n'$  is the slope or apparent SCG parameter and  $\beta$  is the intercept, which can be determined from the numerical results using a linear regression analysis based on equation (21).

The relationship between the calculated apparent SCG parameter  $n'$  and the true SCG parameter  $n$  for  $R = 0.1$  and  $0.5$  showed the following relations with  $r^2 > 0.999$ :

$$\begin{aligned} n' &= 0.9777n + 2.5296 & \text{for } R = 0.1 \\ n' &= 0.9772n + 2.5411 & \text{for } R = 0.5 \end{aligned} \quad (22)$$

Because the difference between  $n'$  and  $n$  was  $\geq 7$  percent for  $n \leq 20$  and  $\leq 3$  percent  $n \geq 40$ , a further approximation of equation (22) can be made for  $R = 0.1$  and  $0.5$  for the case of  $n \geq 40$ :

$$n' \approx n \quad (23)$$

The relationship between  $\beta$  and  $n$  was

$$\begin{aligned} \beta &= 0.1409 + 3.559 e^{-0.0737n} \quad \text{for } R = 0.1 \\ \beta &= 0.1185 + 3.782 e^{-0.0857n} \quad \text{for } R = 0.5 \end{aligned} \quad (24)$$

with the correlation coefficient of  $r^2 \geq 0.991$ .

For the nonnormalized expression, equation (11) can be used to reduce equation (21) to

$$\ln t_f = -n' \frac{\sigma_{\max}}{S_i} + \chi \quad (25)$$

where

$$\chi = \ln\left(\frac{a_i}{A}\right) + \beta \quad (26)$$

Therefore, the parameters  $n'$  and  $\chi$  in cyclic stress loading for a given  $R$ -ratio can be obtained from the slope and intercept by a linear regression analysis of the data of  $\ln t_f$  as a function of  $\sigma_{\max}$  or  $\sigma_{\max}/S_i$ . With  $n'$  calculated, the true SCG parameter  $n$  can be evaluated from equation (22). The SCG parameter  $A$  can be estimated from equation (26) with calculated  $\chi$  and  $\beta$  (eq. (24)) along with known values of  $a_i$ . A notable difference in cyclic stress loading between the power-law and exponential formulations is that in the power-law formulation  $t_f$  is a function of  $\sigma_{\max}$  as seen in equation (3), whereas in the exponential formulation  $\ln t_f$  is a function of  $\sigma_{\max}$  or  $\sigma_{\max}/S_i$  as seen in equation (25). Hence, as in the cases of both constant stress rate (refs. 3 and 4) and constant stress loading, the inert strength of a material must be known in cyclic loading beforehand to determine the major SCG parameter  $n$ , again a definite disadvantage of the exponential formulation as compared with the power-law formulation.

## Experimental Verification

### Constant Stress Testing

Time to failure as a function of applied stress in constant stress testing for various ceramics (refs. 19 to 22 and S.R. Choi, 2000, 1993, and 1991, NASA Glenn Research Center, Cleveland, OH, unpublished work) over a wide range of temperatures is shown in figure 3, where  $\sigma$  was plotted against  $\ln t_f$  in accordance with equation (19) in the exponential formulation.<sup>a</sup> The decrease in time to failure with increasing

---

<sup>a</sup> Time to failure is a dependent variable whereas (maximum) applied stress is an independent variable; thus, ideally the resulting plots should reflect this, as in figures 1 or 2. However, the convention is reversed such that (maximum) applied stress is plotted with respect to time to failure. All figures in figure 3 and those that follow use this convention for generality.

applied stress, which represents the susceptibility to slow crack growth, is dependent on material type and test temperature. The individual SCG parameters  $n$  and  $\chi$  were determined from the slope and intercept by the linear regression analysis of  $\ln t_f$  versus  $\sigma$  based on equation (19), together with inert strength (listed in table I) and the relationship of equation (16). The resulting SCG parameters and the correlation coefficients in regression analysis for individual materials under various test conditions are shown in table II. Figure 4 presents the power-law counterpart plots based on the conventional relation of equation (2). The corresponding SCG parameters  $n$  and  $D$  and the correlation coefficients for the power-law case are also listed in table II. Comparing the results in figures 3 and 4 together with the correlation coefficients in table II reveals no significant difference in data fit between the exponential and power-law formulations: The exponential formulation resulted in as good a data fit as that of the power-law formulation.

TABLE I.— SUMMARY OF SLOW-CRACK-GROWTH (SCG) PARAMETER  $A$  FOR VARIOUS BRITTLE MATERIALS IN CONSTANT STRESS AND CYCLIC STRESS LOADING USING BOTH EXPONENTIAL AND POWER-LAW CRACK-VELOCITY FORMULATIONS

[Data shown have been obtained from previous work (refs. 18 through 22).  
SEPB (single edge precracked beam) technique was used in fracture  
toughness evaluation in accordance with ASTM C1421.]

Material <sup>a</sup>	Test Conditions		Fracture toughness, $K_{IC}$ , MPa/m	Inert strength, <sup>b</sup> $S_i$ , MPa	SCG parameter A, m/s	
	Type of test	Temperature, °C			Formulation	
					Exponential	Power-law
Al <sub>2</sub> O <sub>3</sub>	Constant        ▼	Ambient	3.4	295	5.23×10 <sup>-33</sup>	370
Al <sub>2</sub> O <sub>3</sub> (indented)		Ambient	3.4	196	1.25×10 <sup>-25</sup>	0.73
NCX34 Si <sub>3</sub> N <sub>4</sub>		1200	6.9	805	2.33×10 <sup>-17</sup>	2.20×10 <sup>-3</sup>
NCX34 Si <sub>3</sub> N <sub>4</sub>		1300	6.9	805	3.15×10 <sup>-15</sup>	3.37×10 <sup>-3</sup>
NCX34 Si <sub>3</sub> N <sub>4</sub> (tension)		1200	6.9	633	1.22×10 <sup>-12</sup>	1.43×10 <sup>-5</sup>
NC203 SiC		1300	4.0	655	2.58×10 <sup>-14</sup>	1.90×10 <sup>-3</sup>
Al <sub>2</sub> O <sub>3</sub>		1000	3.4	295	5.53×10 <sup>-12</sup>	.07
Ceralloy 147A Si <sub>3</sub> N <sub>4</sub>		1200	5.8	600	9.53×10 <sup>-12</sup>	3.90×10 <sup>-4</sup>
Ceralloy 147A Si <sub>3</sub> N <sub>4</sub>	▼	1200	5.8	600	3.55×10 <sup>-13</sup>	.02
Al <sub>2</sub> O <sub>3</sub>	Cyclic    ▼	Ambient	3.4	295	1.94×10 <sup>-21</sup>	0.03
Al <sub>2</sub> O <sub>3</sub> (indented)		Ambient	3.4	196	8.02×10 <sup>-24</sup>	2.20
NCX34 Si <sub>3</sub> N <sub>4</sub>		1200	6.9	805	6.92×10 <sup>-19</sup>	2.42×10 <sup>-3</sup>
NCX34 Si <sub>3</sub> N <sub>4</sub>		1300	6.9	805	3.91×10 <sup>-17</sup>	.52

<sup>a</sup>Al<sub>2</sub>O<sub>3</sub> is alumina; Si<sub>3</sub>N<sub>4</sub>, silicon nitride; and SiC, silicon carbide.

<sup>b</sup>Inert strength was determined at ambient temperature in oil for SCG-susceptible materials (alumina) and in air for SCG-insensitive material (including most silicon nitrides and silicon carbides). Previous studies on ultrafast strength behavior of various advanced ceramics at elevated temperatures showed that strength at ultrafast test rates of  $10^4$  to  $10^5$  MPa/sec converged and was close to room-temperature inert counterparts (e.g., ref. 26 in summary). Consequently, as close approximation, room-temperature inert strength was used as elevated-temperature inert strength in evaluating parameter  $A$ . Most inert strength data is quoted from reference 26.

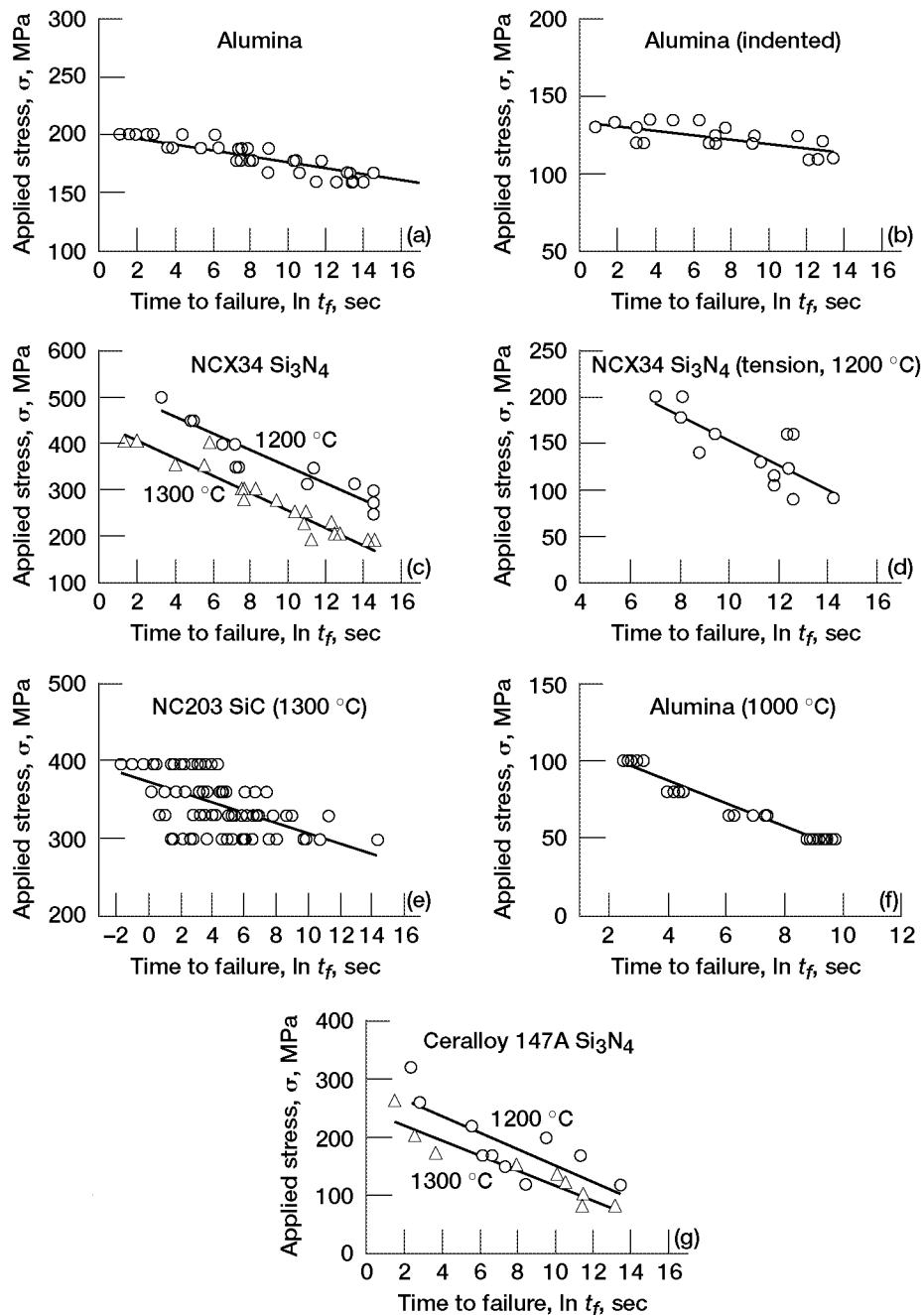


Figure 3.— $\ln$  (time to failure) versus applied stress  $\sigma$  for various ceramics with exponential crack-velocity formulation using equation (19) under constant stress loading. Solid lines represent best fit. (a) Alumina in ambient distilled water in flexure (S.R. Choi, 2000, NASA Glenn Research Center, Cleveland, OH, unpublished work). (b) Alumina (indented) in ambient distilled water in flexure (ref. 19). (c) NCX34 (Norton Co., Worcester, MA) silicon nitride at 1200 and 1300 °C in air in flexure (ref. 20 and S.R. Choi, 1993, NASA Glenn Research Center, Cleveland, OH, unpublished work). (d) NCX34 silicon nitride at 1200 °C in air in tension (ref. 20). (e) NC203 (Norton Co., Worcester, MA) silicon carbide at 1300 °C in air in flexure (ref. 21). (f) Alumina at 1000 °C in air in flexure (ref. 22). (g) Ceralloy 147A (Ceradyne, Inc., Costa Mesa, CA) silicon nitride at 1200 and 1300 °C in air in flexure (S.R. Choi, 1991, NASA Glenn Research Center, Cleveland, OH, unpublished work).

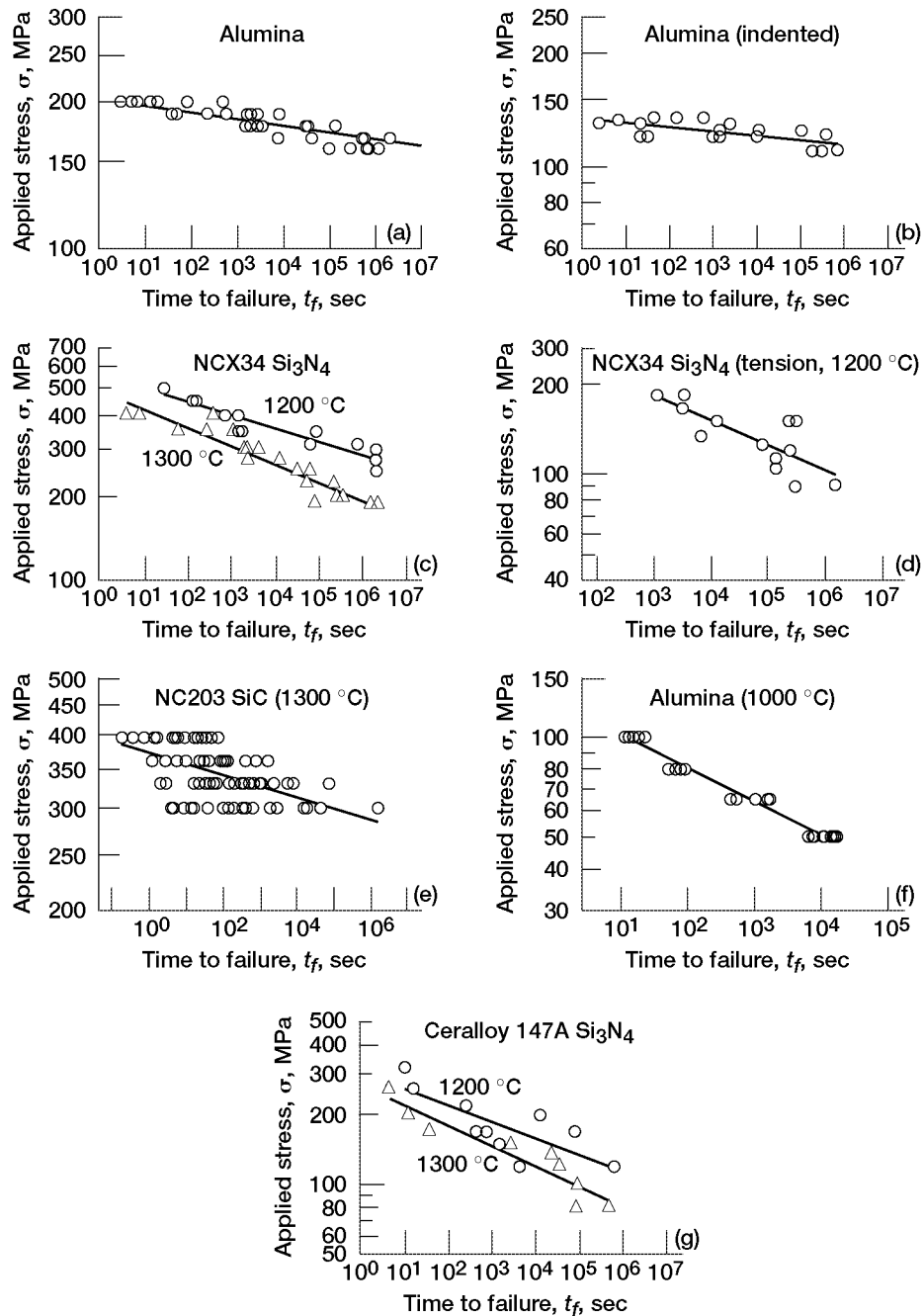


Figure 4.—Time to failure  $t_f$  as function of applied stress  $\sigma$  or various ceramics with power-law crack-velocity formulation using equation (2) under constant stress loading. Solid lines represent best fit. (a) Alumina in ambient distilled water in flexure (S.R. Choi, 2000, NASA Glenn Research Center, Cleveland, OH, unpublished work). (b) Alumina (indented) in ambient distilled water in flexure (ref. 19). (c) NCX34 silicon nitride at 1200 and 1300 °C in air in flexure (ref. 20 and S.R. Choi, 1993, NASA Glenn Research Center, Cleveland, OH, unpublished work). (d) NCX34 silicon nitride at 1200 °C in air in tension (ref. 20). (e) NC203 silicon carbide at 1300 °C in air in flexure (ref. 21). (f) Alumina at 1000 °C in air in flexure (ref. 22). (g) Ceralloy 147A silicon nitride at 1200 and 1300 °C in air in flexure (S.R. Choi, 1991, NASA Glenn Research Center, Cleveland, OH, unpublished work).

TABLE II.—SUMMARY OF SLOW-CRACK-GROWTH (SCG) PARAMETERS AND CORRELATION COEFFICIENTS OF DATA FIT FOR VARIOUS BRITTLE MATERIALS USING BOTH EXPONENTIAL AND POWER-LAW CRACK-VELOCITY FORMULATIONS IN CONSTANT STRESS AND CYCLIC STRESS LOADING

[Mode of tests was in four-point flexure.]

Material <sup>a</sup>	Test conditions		Formulation						Reference
			Exponential			Power-law			
	Type of test	Temperature, <sup>b</sup> °C	SCG parameter, <sup>c</sup> $n_e$	SCG parameter, <sup>d</sup> $\chi$	Correlation coefficient, <sup>e</sup> $r^2$	SCG parameter, $n_p$	Log D <sup>d</sup>	Correlation coefficient, <sup>e</sup> $r^2$	
Al <sub>2</sub> O <sub>3</sub>	Constant        ▼	Ambient	87.6	63.3181	0.7541	54.5	126.7306	0.7538	(f)
Al <sub>2</sub> O <sub>3</sub> (indented)		Ambient	61.0	47.3313	.4367	39.7	86.3279	0.4411	19
NCX34 Si <sub>3</sub> N <sub>4</sub>		1200	37.3	27.4263	.8837	18.5	51.3172	0.8955	20
NCX34 Si <sub>3</sub> N <sub>4</sub>		1300	36.3	22.5133	.9055	13.5	36.7292	0.8988	(g)
NCX34 Si <sub>3</sub> N <sub>4</sub> (tension) <sup>h</sup>		1200	27.0	17.5694	.6278	6.4	18.3751	0.6024	20
NC203 SiC		1300	27.6	20.2295	.3058	7.7	42.2076	0.3013	21
Al <sub>2</sub> O <sub>3</sub>		1000	36.3	15.6789	.9638	15.9	20.3067	0.9798	22
Ceralloy <sup>i</sup> 147A Si <sub>3</sub> N <sub>4</sub>		1200	22.9	15.5657	.6094	9.6	22.5671	0.6051	(j)
Ceralloy <sup>i</sup> 147A Si <sub>3</sub> N <sub>4</sub>	▼	1300	38.8	17.9811	.8927	8.6	25.0071	0.8860	(j)
Al <sub>2</sub> O <sub>3</sub>	Cyclic    ▼	Ambient	45.9	38.7877	0.6299	10.1	77.5788	0.6356	23
Al <sub>2</sub> O <sub>3</sub> (indented)		Ambient	59.5	44.7325	.7936	32.5	77.4315	0.7925	19
NCX34 Si <sub>3</sub> N <sub>4</sub>		1200	41.6	32.0421	.8027	20.8	58.5654	0.7815	24
NCX34 Si <sub>3</sub> N <sub>4</sub>		1300	52.3	27.9453	.7872	17.5	46.8061	0.7631	(g)

<sup>a</sup>Al<sub>2</sub>O<sub>3</sub> is alumina, Si<sub>3</sub>N<sub>4</sub> is silicon nitride, and SiC is silicon carbide.

<sup>b</sup>Testing at ambient temperature was performed in distilled water.

<sup>c</sup>Inert strength listed in table II was used in calculating  $n$  in exponential formulation.

<sup>d</sup>SCG parameters  $\chi$  and  $D$  were determined with units of time to failure in seconds and stress in megapascals.

<sup>e</sup> $r^2$  indicates square of correlation coefficient.

<sup>f</sup>S.R. Choi, 2000, NASA Glenn Research Center, Cleveland, OH, unpublished work.

<sup>g</sup>S.R. Choi, 1993, NASA Glenn Research Center, Cleveland, OH, unpublished work.

<sup>h</sup>Tests for NCX34 (tension) were performed in tension rather than in flexure.

<sup>i</sup>Ceradyne, Inc., Costa Mesa, CA.

<sup>j</sup>S.R. Choi, 1991, NASA Glenn Research Center, Cleveland, OH, unpublished work.



## Cyclic Stress Testing

Figure 5 shows previous results of cyclic stress testing for alumina and NCX34 silicon nitride (refs. 19, 23, 24, and S.R. Choi, 1993, NASA Glenn Research Center, Cleveland, OH, unpublished work) where  $\sigma_{\max}$  was plotted against  $\ln t_f$  based on equation (25) in the exponential formulation for each material under given test conditions.<sup>a</sup> As in constant stress testing, the materials exhibited the decrease in time to failure with increasing maximum applied stress, indicative of susceptibility to SCG. The SCG parameters  $n$  and  $\chi$  were determined from the slope and intercept by linear regression of  $\ln t_f$  versus  $\sigma_{\max}$ , based on equation (25) together with inert strength (listed in table I) and the relationship of equation (22). The SCG parameters thus evaluated and the correlation coefficients in regression analysis are listed in table II. Figure 6 presents the counterpart plots of the experimental data using the power-law formulation (equation (3)). Similar to the case of constant stress testing, there was no significant difference in data fit between the exponential and power-law formulations. Hence, both the exponential and power-law formulations would give an equally reasonable data fit, so a choice of SCG formulations would not make any difference in terms of the degree of data fit.

## Discussion

### Relationship Between SCG Parameters $n$

Because of the functional form of the crack-velocity equation in either the exponential or power-law formulation, the SCG parameter  $n$  has the most sensitive and significant effect on lifetime; thus, accurate estimation of  $n$  is crucially important and must always be emphasized. In fact,  $n$  in the conventional power-law formulation has been used as an important measure of SCG susceptibility of brittle materials: There is significant SCG susceptibility for  $n < 30$ , intermediate susceptibility for  $n = 30$  to 50, and insignificant (or highly resistant to SCG) susceptibility for  $n > 50$ . Therefore, it is worthwhile to establish the relationship of  $n$  in the exponential formulation to that in the power-law formulation, which can be done using the  $n$  values from table II determined in constant stress and cyclic stress testing. Figure 7 illustrates the relationship between the SCG parameters  $n$  from each formulation. The overall relationship with a total of 13 data points was approximated as follows:

$$n_e = 1.110n_p + 19.957 \quad (27)$$

with a correlation coefficient of  $r^2 = 0.8439$ . The  $n_e$  and  $n_p$  represent the SCG parameter  $n$  in exponential and power-law formulations, respectively. The  $n_e$  is greater than  $n_p$  by approximately 20. Figure 7 also includes the relationship determined from the data in constant stress rate testing (ref. 4), where the corresponding relationship was

$$n_e = 0.964n_p + 12.524 \quad (28)$$

with  $r^2 = 0.9511$ . Hence, the two relationships (eqs. (27) and (28)) were not in good agreement, resulting in a difference of about 10 in the values of  $n_e$  between them.

This difference in  $n$  can be seen more easily if  $n$  in constant stress rate loading is plotted against that in constant stress and cyclic loading, which is shown in figure 8. Although the overall relationship between  $n$  in constant stress rate loading and  $n$  in constant stress and/or cyclic loading seems to be 1:1 in the exponential formulation (fig. 8(a)), the data scatter was significant with a tendency of  $n$  to be greater in constant stress and cyclic loading than in constant stress rate loading. The corresponding

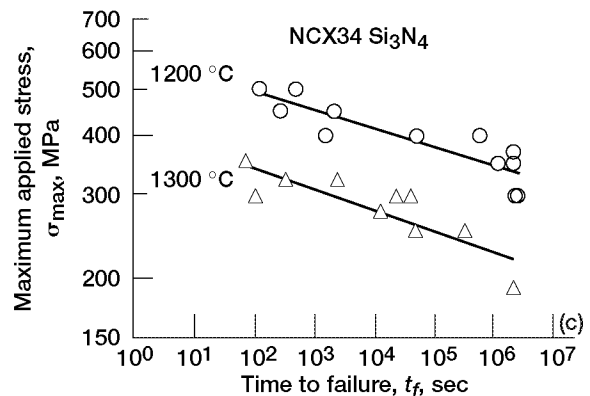
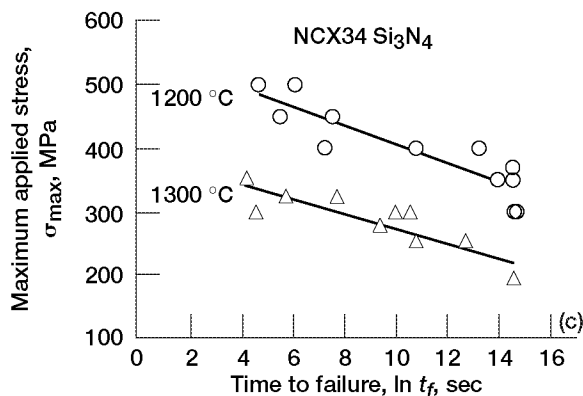
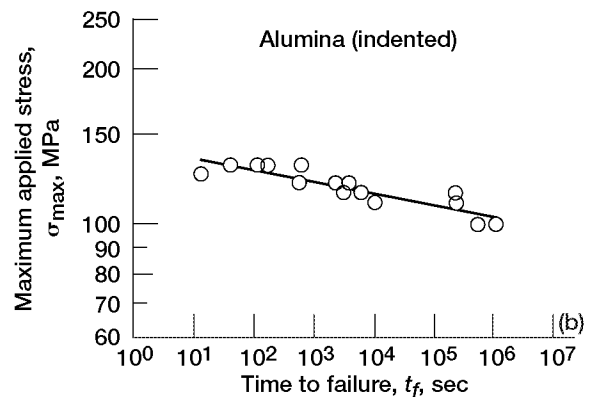
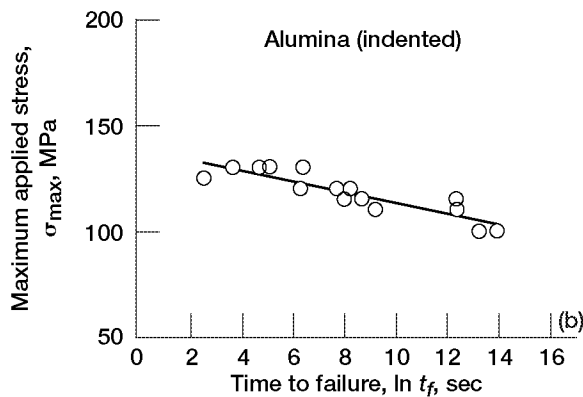
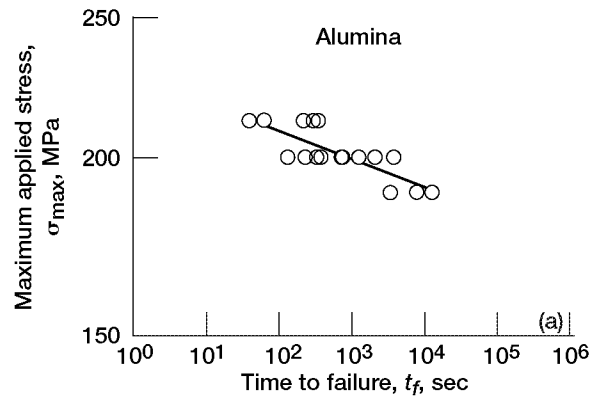
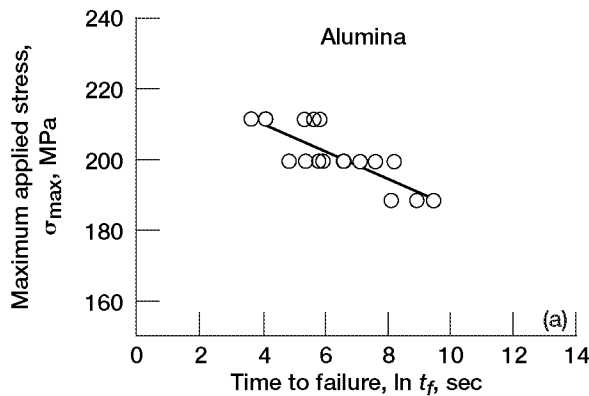


Figure 5.—ln (time to failure) versus maximum applied stress in exponential crack-velocity formulation using equation (25) under sinusoidal cyclic loading. Solid lines represent best fit. (a) Alumina in ambient distilled water in flexure ( $R = 0.1$ ) (ref. 23). (b) Alumina (indented) in ambient distilled water in flexure ( $R = 0.5$ ) (ref. 19). (c) NCX34 silicon nitride at 1200 (ref. 24) and 1300 °C (S.R. Choi, 1993, NASA Glenn Research Center, Cleveland, OH, unpublished work) in air in flexure ( $R = 0.5$ ).

Figure 6.—log (time to failure) versus log (maximum applied stress) for various ceramics with power-law crack-velocity formulation using equation (3) under sinusoidal cyclic loading. Solid lines represent best fit. (a) Alumina in ambient distilled water in flexure ( $R = 0.1$ ) (ref. 23). (b) Alumina (indented) in ambient distilled water in flexure ( $R = 0.5$ ) (ref. 19). (c) NCX34 silicon nitride at 1200 °C (ref. 24) and 1300 °C (S.R. Choi, 1993, NASA Glenn Research Center, Cleveland, OH, unpublished work) in air in flexure ( $R = 0.5$ ).

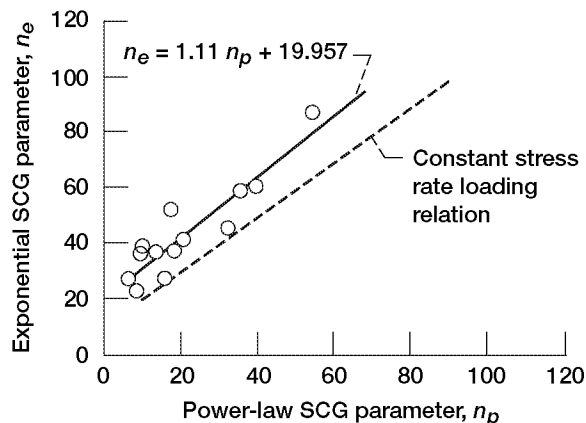


Figure 7.—Relationship of slow-crack-growth (SCG) parameter of exponential formulation  $n_e$  to that of power-law formulation  $n_p$  for various materials from table II for constant stress and cyclic loading. Relationship determined for constant stress rate loading (ref. 4) included for comparison.

relationship in the power-law formulation (fig. 8(b)), however, yields good agreement between constant stress rate loading and constant-stress/cyclic loading, which has been typical of many advanced ceramics observed at Glenn for decades. The reason for less agreement in the exponential formulation is not yet clear and requires more data. It is believed to result from inaccurate values of inert strength of the materials because the SCG parameter  $n$  is determined from both the slope of the time to failure versus stress relation (regression analysis) and the inert strength (eq. (19) or (25)). Note that  $n$  in the power-law formulation is determined solely from the slope of the relations with stress (eq. (2) or (3)).

### SCG Parameter $A$ and Crack Velocity

The parameter  $A$  can be determined using experimental data based on equations (20) and (26) for constant stress and cyclic stress loading, respectively, in the exponential formulation, whereas the respective parameter  $A$  in the power-law formulation can be determined from equations (4) and (5) with the  $B$  expression. The initial crack size or the critical crack size in the inert condition  $a_i$  can be estimated using the fundamental relation of  $K_{IC} = Y S_i a_i^{1/2}$ , assuming the crack configuration to be a semicircle ( $Y = 2/\sqrt{\pi}$ ) and the crack size to be small compared with components or test coupons (i.e., an infinite-body approach). The resulting  $A$  parameters for each material thus estimated for both the exponential and power-law formulations are shown in table I. Unlike the SCG parameter  $n$ , no definite relationship existed for  $A$  between the two formulations, which was similar to that observed in constant stress rate loading (ref. 4). Notwithstanding, the actual crack velocities for a given stress intensity factor seem not much different from each other with some exceptions, as can be seen from the results of  $\log v$  versus  $K_I/K_{IC}$  in figure 9. Each crack velocity for a given  $K_I/K_{IC}$  was calculated using  $A$  and  $n$  from their respective crack-velocity formulas—equation (6) for the exponential formulation and equation (1) for the power-law formulation.

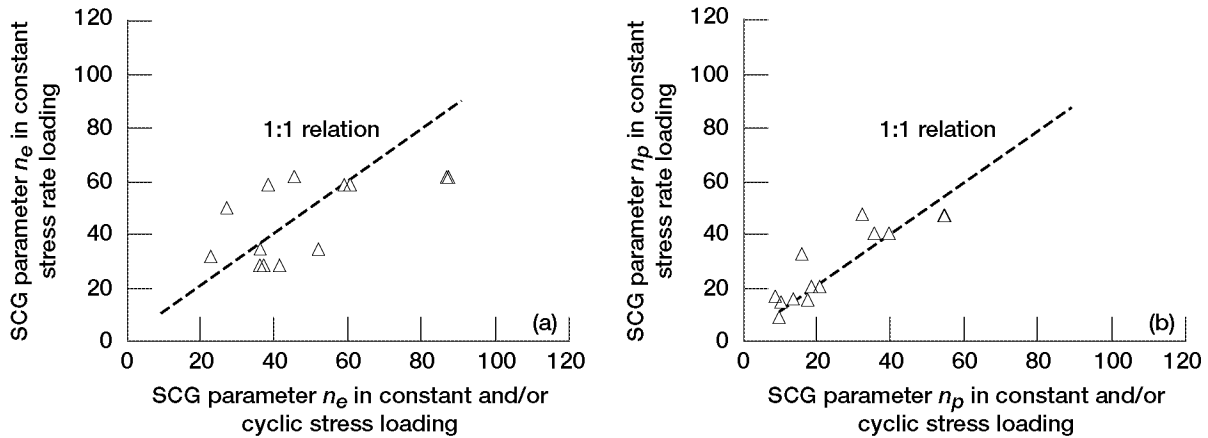


Figure 8.—Relationship between slow-crack-growth (SCG) parameters  $n$  in constant stress rate loading and those in constant stress and/or cyclic stress loading. SCG parameters  $n$  for constant stress-rate loading were obtained from previous study (ref. 4). (a) Exponential crack-velocity formulation. (b) Power-law crack-velocity formulation.

### Life Prediction From Static Loading to Cyclic Loading

The ratio of constant stress to cyclic stress lives,  $h$ -ratio, for the condition of  $\sigma$  in constant stress loading equal to  $\sigma_{\max}$  in cyclic stress loading ( $\sigma = \sigma_{\max}$ ) has been frequently used in the power-law formulation (refs. 6, 18, and 25) to compare lives of static and cyclic loading or to predict life from one loading configuration to another. The  $h$ -ratio is defined as

$$h = \frac{t_{fs}}{t_{fc}} \quad (29)$$

where  $t_{fs}$  and  $t_{fc}$  are times to failure, respectively, in constant stress and cyclic stress loading. The  $h$ -ratio in the exponential formulation has been numerically determined in cyclic loading with different  $R$ -ratios as a function of  $n$  from a previous study (ref. 3), and its results are presented in figure 10(a). The  $h$ -ratio decreases with increasing SCG parameter  $n$ , and the rate of decrease with increasing  $n$  is almost the same regardless of the  $R$ -ratio up to 0.9. Also for a given  $n$ , the  $h$ -ratio increases with increasing  $R$ -ratio. Note that the ratio of  $R = 1.0$  represents the case for constant stress loading. The  $h$ -ratio varies slightly by a factor of 2 for  $\sigma_{\max}^*$  between 0.2 and 0.9: the lower  $\sigma_{\max}^*$  yields the higher  $h$ -ratio and vice versa. Hence, for a conservative estimation, the higher value of  $\sigma_{\max}^* = 0.7$  was used in the calculation of  $h$ -ratio (ref. 3). A very similar trend in  $h$ -ratio was also found previously in the power-law formulation, as shown in figure 10(b) (ref. 18). Unlike the exponential formulation, the power-law formulation revealed no effect of  $\sigma_{\max}^*$  on the  $h$ -ratio for a given  $R$ -ratio.

Figure 11(a) shows examples of lives predicted from the constant stress data (fig. 3) for a cyclic loading configuration for alumina at ambient temperature and for NCX34 silicon nitride at elevated temperatures using the solution shown in figure 10(a). The prediction did not seem to be in good agreement with the actual cyclic stress data. However, if one considers that scatter in time to failure in either constant stress or cyclic stress testing for most machined ceramics is usually significant, typically 2 or 3 orders of magnitude, the prediction and the experimental data are in reasonable agreement since the deviation is still within 1 order of magnitude. The counterpart plots of prediction using the power-law formulation (fig. 10(b)) are shown in figure 12. By comparing figures 11 and 12, one can conclude readily that the exponential and the power-law formulations result in almost the same degree of accuracy in life prediction for each given material and test conditions.

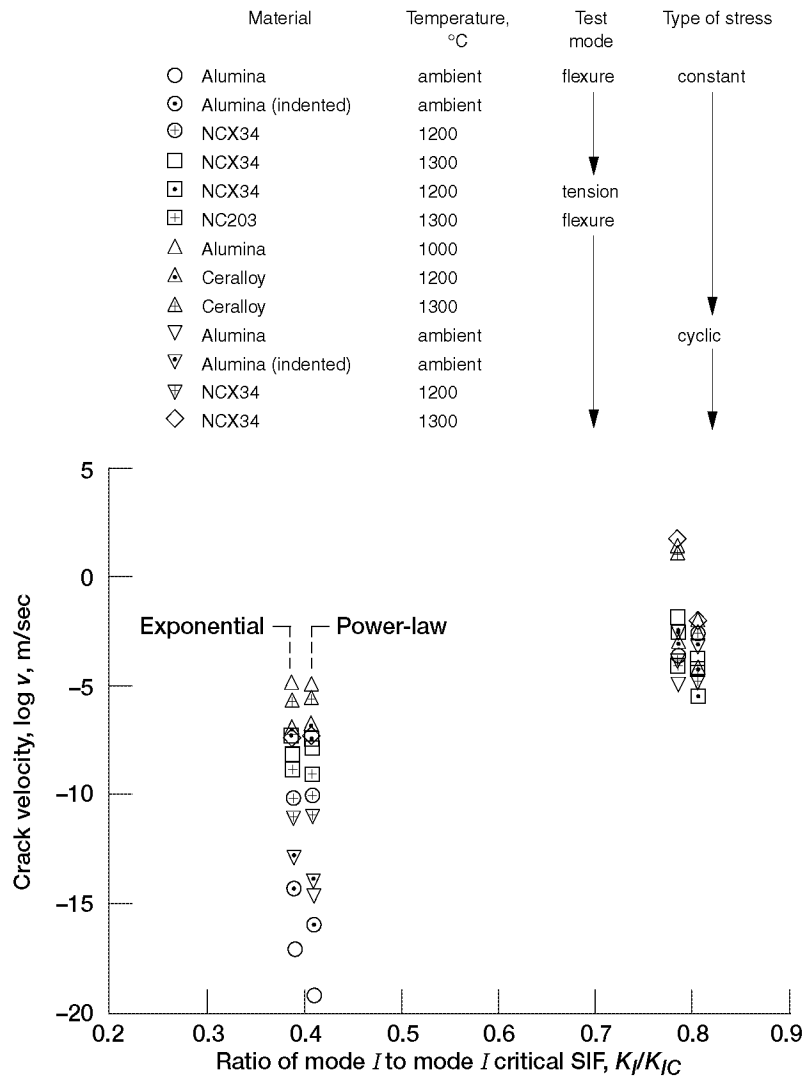


Figure 9.—Comparison of crack velocity as function of stress intensity factor (SIF)  $K_I/K_{IC}$  in both exponential and power-law formulations for materials used in this report.

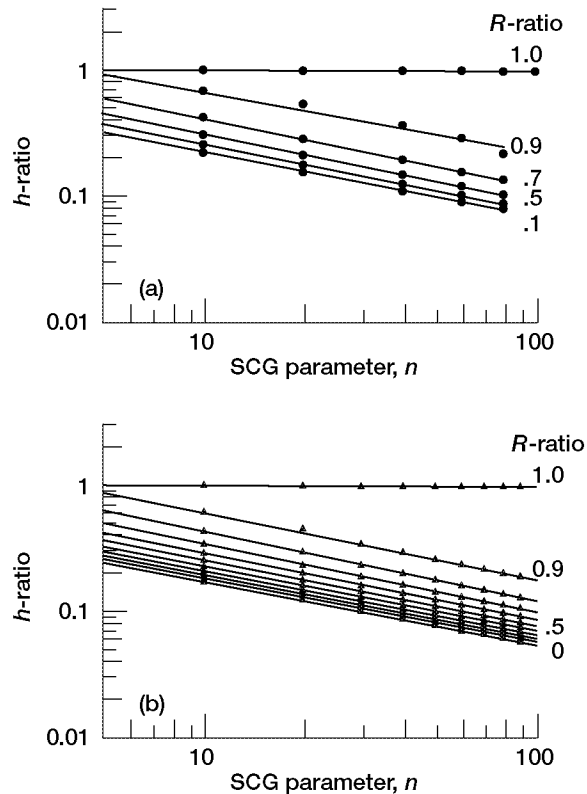


Figure 10.— $h$ -ratio as function of SCG parameter  $n$  for different values of  $R$ -ratio. Each line represents best fit. (a) Exponential crack-velocity formulation (ref. 3). (b) Power-law crack-velocity formulation (ref. 18).

### Limitation of Exponential Formulation

Although the exponential formulations used to determine SCG parameters required somewhat inconvenient numerical procedures (ref. 3), their resulting solutions under a constant stress rate loading condition had shown to yield almost the same degree of simplicity in data analysis as well as in the agreement in experimental data as those in the power-law formulation (ref. 4). The same was true for constant stress and cyclic stress loading conditions, as appeared from the present results. However, that the inert strength of a material must be known beforehand to determine the major SCG parameter  $n$  can be a major drawback and/or obstacle in using the exponential formulation in terms of simplicity and accuracy, as compared with the power-law formulation, which does not require knowledge of the inert strength. Inert strength of a material at room temperature, of course, is not difficult to determine; however, even in this case care must be exercised to provide a perfect inert condition by using appropriate conditions (environment and test rate) so that an accurate inert strength can be evaluated. A greater burden would be determining inert strength at elevated temperatures, although the authors have done pioneering work in this subject using a total 17 advanced ceramics (see ref. 26 for summary) with some conclusive results that the elevated-temperature inert strength of a ceramic material can be estimated with an ultrafast test rate of  $\geq 10^5$  MPa/sec and that the elevated-temperature inert strength is close to that of the room-temperature. However, this finding has not yet been finalized, and a more valid data base needs to be established.

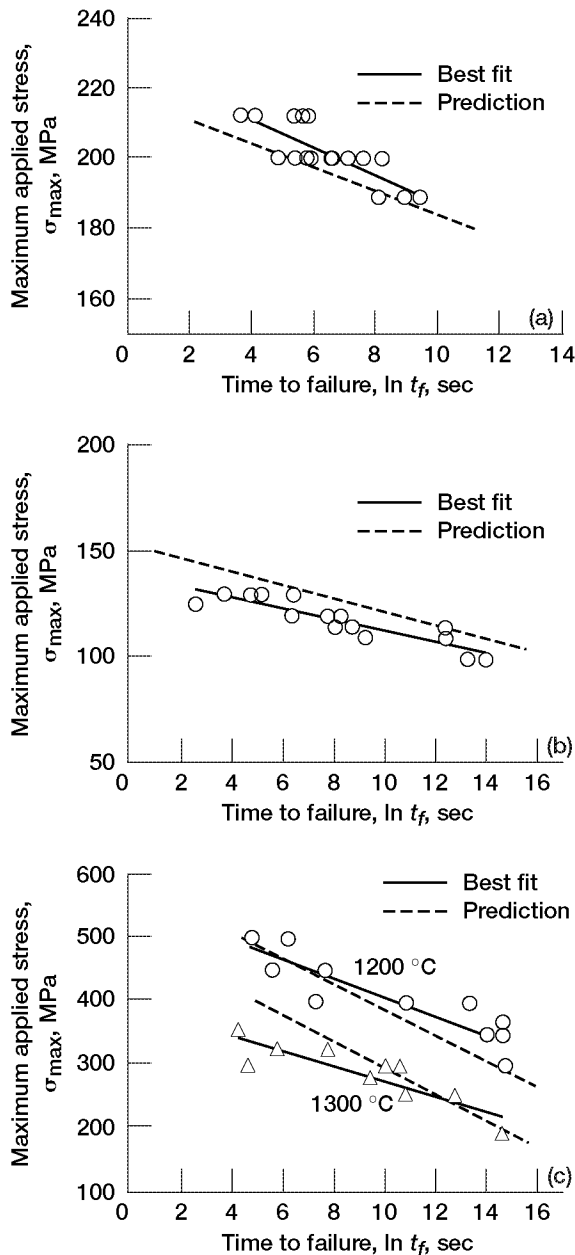


Figure 11.—Life prediction in sinusoidal cyclic loading from constant stress loading data with exponential crack-velocity formulation (eq. (28) and fig. 10 (a)). (a) Alumina in ambient distilled water in flexure (ref. 26 and S.R. Choi, 2000, NASA Glenn Research Center, Cleveland, OH, unpublished work).  $R = 0.1$ . (b) Alumina (indented) in ambient distilled water in flexure (ref. 20).  $R = 0.5$ . (c) NCX34 silicon nitride at 1200 and 1300 °C in air in flexure (refs. 20, 24, and S.R. Choi, 1993 and 1991, NASA Glenn Research Center, Cleveland, OH, unpublished work).  $R = 0.5$ .

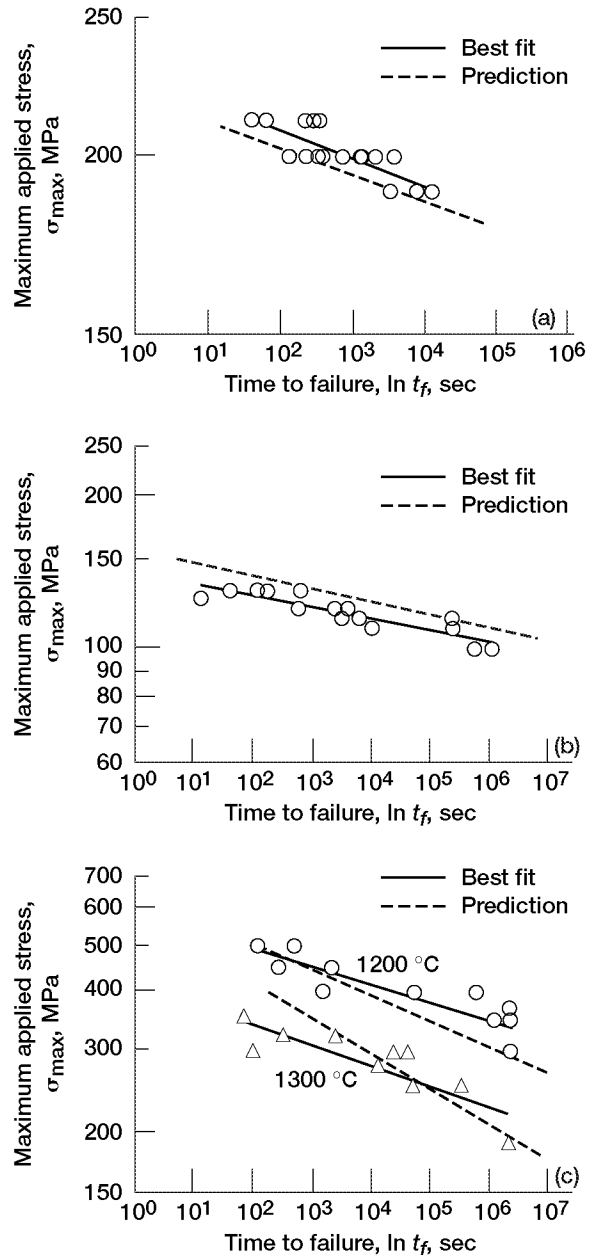


Figure 12.—Life prediction in sinusoidal cyclic loading from constant stress loading data with power-law crack-velocity formulation (eq. (28) and fig. 10 (b)). (a) Alumina in ambient distilled water in flexure (ref. 26 and S.R. Choi, 2000, NASA Glenn Research Center, Cleveland, OH, unpublished work).  $R = 0.1$ . (b) Alumina (indented) in ambient distilled water in flexure (ref. 19).  $R = 0.5$ . (c) NCX34 silicon nitride at 1200 and 1300 °C in air in flexure (refs. 20, 24, and S.R. Choi, 1993 and 1991, NASA Glenn Research Center, Cleveland, OH, unpublished work).  $R = 0.5$ .

## Conclusions

1. The data fit to the  $\ln$  (*time to failure*) versus (*maximum*) *applied stress* relation in the exponential crack-velocity formulation under constant stress or cyclic stress loading was found very reasonable for most of the advanced ceramics used.

2. The relationship of slow-crack-growth (SCG) parameters  $n$  determined with the exponential formulation  $n_e$ , to those determined with the power-law formulation  $n_p$  was comparable under both constant stress and cyclic stress loading. However, this relationship was not similar to those determined under constant stress rate loading.

3. Life prediction in the cyclic stress loading configuration from constant stress loading data was in good agreement with the actual cyclic stress experimental data. The prediction in the exponential formulation was almost identical in terms of accuracy to that in the power-law formulation.

4. Despite little difference both in the data fit from one loading configuration to another, the major limitation in the requirement of knowledge of inert strength in evaluating the SCG parameter  $n$  makes the power-law formulation a more preferable choice for life prediction and SCG parameter determination than the exponential formulation.



## Appendix—Symbols

$A$	slow-crack-growth parameter defined in equations (1) and (6)
$a$	crack size
$B$	slow-crack-growth parameter, $B = 2K_{IC}/[AY^2(n - 2)]$
$C$	crack size in normalized scheme of references 16 to 18
$D$	slow-crack-growth parameter defined in equations (4) and (5)
$f(t)$	periodic function, cyclic loading
$h$	ratio of constant to cyclic stress loading lifetimes
$K$	stress intensity factor
$n$	slow-crack-growth parameter defined in equations (1) and (6)
$R$	stress ratio
$r^2$	correlation coefficient
$S$	strength, MPa
$T$	time in normalized scheme of references 16 to 18
$t$	time, sec
$v$	crack velocity
$Y$	crack geometry factor
$\beta$	intercept of curve in linear regression analysis
$\chi$	slow-crack-growth parameter defined in equation (20)
$\sigma$	applied stress, MPa
$\tau$	period
$\omega$	angular velocity

Subscripts:

$C$           critical

$c$	cyclic stress
$e$	exponential formulation
$f$	fracture
$I$	mode I
$i$	inert or initial condition
max	maximum
min	minimum
$p$	power-law formulation
$s$	constant stress

Superscripts:

*	normalized
'	apparent (calculated)

## References

1. Standard Test Method for Determination of Slow Crack Growth Parameters of Advanced Ceramics by Constant Stress-Rate Flexural Testing at Ambient Temperature. Annual Book of ASTM Standards 2001, ASTM Designation: C 1368-00, sec. 15, vol. 15.01, ASTM, West Conshohocken, PA, 2001, pp. 626-634.
2. Standard Test Method for Determination of Slow Crack Growth Parameters of Advanced Ceramics by Constant Stress-Rate Flexural Testing at Elevated Temperatures. Annual Book of ASTM Standards 2001, ASTM Designation: C 1465-00, sec. 15, vol. 15.01, ASTM, West Conshohocken, PA, 2001, pp. 703-716.
3. Choi, S.R.; Nemeth, N.N.; and Gyekenyesi, J.P.: Slow Crack Growth of Brittle Materials With Exponential Crack Velocity Formulation—Part 1: Analysis. NASA/TM—2002-211153-1.
4. Choi, S.R.; Nemeth, N.N.; and Gyekenyesi, J.P.: Slow Crack Growth of Brittle Materials With Exponential Crack Velocity Formulation—Part 2: Constant Stress Rate Experiments. NASA/TM—2002-211153-2.
5. Ritter, John E., Jr.: Engineering Design and Fatigue Failure of Brittle Materials. Fracture Mechanics of Ceramics, R.C. Bradt, D.P.H. Hasselman, and F.F. Lange, eds., vol. 4, Plenum Press, New York, NY, 1978, pp. 667-686.
6. Evans, A.G.; and Fuller, E.R.: Crack Propagation in Ceramic Materials Under Cyclic Loading Conditions. Metall. Trans., vol. 5, no. 1, 1974, pp. 27-33.
7. Hillig, W.B.; and Charles, R.J.: Surfaces, Stress-Dependent Surface Reactions, and Strength. High Strength Materials, Victor F. Zackay, ed., ch. 17, John Wiley & Sons, Inc., New York, NY, pp. 682-705.
8. Charles, R.J.: Diffusion Controlled Stress Rupture of Polycrystalline Materials. Metall. Trans. A, vol. 7A, no. 8, 1976, pp. 1081-1089.
9. Pollet, J.-C.; and Burns, S.J.: Thermally Activated Crack Propagation—Theory. Int. J. Fracture, vol. 13, no. 5, 1977, pp. 667-679.
10. Wiederhorn, S.M.; and Bolz, L.H.: Stress Corrosion and Static Fatigue of Glass. J. Am. Ceram. Soc., vol. 53, no. 10, 1970, pp. 543-548.
11. Lawn, B.R.: An Atomistic Model of Kinetic Crack Growth in Brittle Solids. J. Mater. Sci., vol. 10, 1975, pp. 469-480.
12. Lenoe, E.M.; and Neal, D.M.: Assessment of Strength-Probability-Time Relationships in Ceramics. ARPA Order 2181, AMMRC-TR-75-13, 1975.
13. Trantina, G.G.: Strength and Life Prediction for Hot-Pressed Silicon Nitride. J. Am. Cer. Soc., vol. 62, no. 7-8, 1979, pp. 377-380.
14. Ritter, John E., et al.: Dynamic Fatigue Analysis of Indentation Flaws Using an Exponential-Law Crack Velocity Function. Commun. Am. Ceram. Soc., 1984, pp. C-198—C-199.
15. Ritter, John E., Jr.; Jakus, Karl; and Cooke, David S.: Predicting Failure of Optical Glass Fibers. Environmental Degradation of Engineering Materials in Aggressive Environments, Proceedings of Second International Conference on Environmental Degradation of Engineering Materials, 1981, pp. 565-575.
16. Lawn, B.R., et al.: Fatigue Analysis of Brittle Materials Using Indentation Flaws. J. Mat. Sci., pt. 1, vol. 16, no. 10, 1981, pp. 2846-2854.
17. Choi, S.R.; Ritter, J.E.; and Jakus, K.: Failure of Glass With Subthreshold Flaws. J. Am. Ceram. Soc., vol. 73, no. 2, 1990, pp. 268-274.
18. Choi, Sung R.; and Salem, Jonathan A.: Cyclic Fatigue of Brittle Materials With an Indentation-Induced Flaw System. Mater. Sci. Eng. A, vol. A208, 1996, pp. 126-130.
19. Choi, S.R.; and Salem, J.A.: Dynamic, Static and Cyclic Fatigue of Alumina With Indentation-Induced Flaws. J. Mater. Sci. Lett., vol. 14, 1995, pp. 1286-1288.

20. Choi, Sung R.; Salem, Jonathan A.; and Palko, Joseph L.: Comparison of Tension and Flexure to Determine Fatigue Life Prediction Parameters at Elevated Temperatures. ASTM STP 1201, C.R. Brinkman and S.F. Duffy, eds., ASTM, Philadelphia, PA, 1994.
21. Choi, Sung R.; Salem, J.A.; and Nemeth, N.N.: High-Temperature Slow Crack Growth of Silicon Carbide Determined by Constant-Stress-Rate and Constant-Stress Testing. *M. Mater. Sci.*, vol. 33, 1998, pp. 1325–1332.
22. Choi, S.R.; and Gyekenyesi, J.P.: Slow Crack Growth Analysis of Advanced Structural Ceramics Under Combined Loading Conditions: Damage Assessment in Life Prediction Testing. *J. Eng. Gas Turbines Power*, vol. 123, 2001, pp. 277–287.
23. Choi, Sung R.; and Salem, Jonathan A.: Error in Flexure Testing of Advanced Ceramics Under Cyclic Loading. *Ceramic Engineering & Science Proceedings*, vol. 18, issue 3, 1997, pp. 495–502.
24. Choi, Sung R., et al.: Elevated Temperature Slow Crack Growth of Silicon Nitride Under Dynamic, Static and Cyclic Flexural Loading. *Ceramic Engineering & Science Proceedings*, 1994, pp. 597–604.
25. Kawakubo, T.; and Komeya, K.: Static and Cyclic Fatigue Behavior of a Sintered Silicon-Nitride at Room-Temperature. *J. Am. Ceram. Soc.*, vol. 70, no. 6, 1987, pp. 400–405.
26. Choi, Sung R.; and Gyekenyesi, John P.: “Ultra”-Fast Fracture Strength of Advanced Structural Ceramics at Elevated Temperatures: An Approach to High-Temperature ‘Inert’ Strength. *Fracture Mechanics of Ceramics*, R.C. Bradt et al., eds., Vol. 13, Kluwer Academic/Plenum Publishers, New York, NY, 2002, pp. 27–46.

REPORT DOCUMENTATION PAGE			Form Approved OMB No. 0704-0188	
Public reporting burden for this collection of information is estimated to average 1 hour per response, including the time for reviewing instructions, searching existing data sources, gathering and maintaining the data needed, and completing and reviewing the collection of information. Send comments regarding this burden estimate or any other aspect of this collection of information, including suggestions for reducing this burden, to Washington Headquarters Services, Directorate for Information Operations and Reports, 1215 Jefferson Davis Highway, Suite 1204, Arlington, VA 22202-4302, and to the Office of Management and Budget, Paperwork Reduction Project (0704-0188), Washington, DC 20503.				
1. AGENCY USE ONLY (Leave blank)	2. REPORT DATE July 2002	3. REPORT TYPE AND DATES COVERED Technical Memorandum		
4. TITLE AND SUBTITLE  Slow Crack Growth of Brittle Materials With Exponential Crack-Velocity Formulation—Part 3: Constant Stress and Cyclic Stress Experiments		5. FUNDING NUMBERS  WU-708-31-13-00		
6. AUTHOR(S)  Sung R. Choi, Noel N. Nemeth, and John P. Gyekenyesi				
7. PERFORMING ORGANIZATION NAME(S) AND ADDRESS(ES)  National Aeronautics and Space Administration John H. Glenn Research Center at Lewis Field Cleveland, Ohio 44135-3191		8. PERFORMING ORGANIZATION REPORT NUMBER  E-13009-3		
9. SPONSORING/MONITORING AGENCY NAME(S) AND ADDRESS(ES)  National Aeronautics and Space Administration Washington, DC 20546-0001		10. SPONSORING/MONITORING AGENCY REPORT NUMBER  NASA TM-2002-211153-PART3		
11. SUPPLEMENTARY NOTES  Sung R. Choi, Ohio Aerospace Institute, Brook Park, Ohio 44142; Noel N. Nemeth and John P. Gyekenyesi, NASA Glenn Research Center. Responsible person, Sung R. Choi, organization code 5920, 216-433-8366.				
12a. DISTRIBUTION/AVAILABILITY STATEMENT  Unclassified - Unlimited Subject Categories: 07 and 39 Available electronically at <a href="http://gltrs.grc.nasa.gov/GLTRS">http://gltrs.grc.nasa.gov/GLTRS</a> This publication is available from the NASA Center for AeroSpace Information, 301-621-0390.			12b. DISTRIBUTION CODE	
13. ABSTRACT (Maximum 200 words)  The previously determined life prediction analysis based on an exponential crack-velocity formulation was examined using a variety of experimental data on advanced structural ceramics tested under constant stress and cyclic stress loading at ambient and elevated temperatures. The data fit to the relation between the time to failure and applied stress (or maximum applied stress in cyclic loading) was very reasonable for most of the materials studied. It was also found that life prediction for cyclic stress loading from data of constant stress loading in the exponential formulation was in good agreement with the experimental data, resulting in a similar degree of accuracy as compared with the power-law formulation. The major limitation in the exponential crack-velocity formulation, however, was that the inert strength of a material must be known a priori to evaluate the important slow-crack-growth (SCG) parameter $n$ , a significant drawback as compared with the conventional power-law crack-velocity formulation.				
14. SUBJECT TERMS  Slow crack growth analysis; Life prediction; Brittle materials; Ceramics and glass; Life prediction testing; Mechanical testing			15. NUMBER OF PAGES 30	
			16. PRICE CODE	
17. SECURITY CLASSIFICATION OF REPORT Unclassified	18. SECURITY CLASSIFICATION OF THIS PAGE Unclassified	19. SECURITY CLASSIFICATION OF ABSTRACT Unclassified	20. LIMITATION OF ABSTRACT	